Comprehensive Data-Driven Framework for Statistical Transient Stability Analysis in Variable Inertia Power Systems Enabled by High-Throughput Simulation

Keito Nishida
Graduate School of Engineering
University of Fukui
Fukui, Japan
nkd23006@u-fukui.ac.jp

Ryuto Shigenobu
Faculty of Engineering
University of Fukui
Fukui, Japan
lute@u-fukui.ac.jp
0000-0001-8106-074X

Akiko Takahashi
Faculty of Basic and Generic Researches
University of Fukui
Fukui, Japan
takahasi@u-fukui.ac.jp

Masakazu Ito
Faculty of Engineering
University of Fukui
Fukui, Japan
itomasa@u-fukui.ac.jp
0000-0002-8932-4014

***Abstract*— The integration of renewable energy reduces electrical power system inertia, increasing vulnerability to disturbances. Conventional transient stability analysis suffers from event selectivity limitations. Hence, predetermined "worst case" scenarios overlook the risk associated with critical vulnerability patterns. This paper demonstrates that high-throughput simulation can systematically explore the entire contingency pattern to identify essential clusters of vulnerability. The automated framework reduces simulation time by 85% while enabling statistical analysis across different inertia levels (2s, 8s, 16s) and disturbance magnitudes (250-1000 MW) using the IEEJ EAST 10-machine system. The RoCoF and Nadir results reveal distinct spatial vulnerability clustering, with buses 18, 19, 20, 36, 37, and 47 consistently exhibiting the highest impacts regardless of operating conditions. These topology-dependent vulnerability patterns require comprehensive rather than selective analysis for practical power system security assessment.**

Keywords — transient stability analysis, data-driven, high-throughput simulation, contingency, inertia, RoCoF, Nadir

I. Introduction

The energy transition is fundamentally altering the topology of the electrical power system through the displacement of conventional synchronous generators with inverter-based resources (IBRs) [1, 2, 3, 4]. This inevitable transition reduces system inertia and resilience, consequently leading to faster frequency fluctuations and increased vulnerability to disturbances [5, 6]. The 2016 South Australian blackout exemplifies the risks associated with such low-inertia systems [7]. Thus, modern electrical power systems face challenges mentioned above as the integration of renewable energy accelerates, driven by climate policies and technological advancements [8, 9].

While past contingency event analysis can focus on the specific situation that has already occurred, on the other hand, analysis of future events faces a fundamentally different and more challenging problem [10]. For a future event, it is necessary to predict which events might occur and assess their potential impacts. However, the number of events must be enormous, making comprehensive analysis seemingly intractable. In other words, conventional transient stability analysis suffers from a critical limitation known as event selectivity. Specifically, selected events are referred to as worst-case scenarios, a predetermined subset of possible contingencies [11, 12, 13]. However, when the future contingencies remain unknown and the total contingency space is vast, it becomes unclear which events truly constitute the "worst case" scenarios for ensuring comprehensive system security. Consequently, analyzing only a limited number of pre-selected events is insufficient to draw definitive conclusions. Therefore, generating comprehensive datasets through high-throughput simulation is necessary. This countermeasure enables systematic exploration of the entire contingency space, thereby eliminating the uncertainty inherent in selective event analysis.

Therefore, this paper proposes a comprehensive data-driven approach to overcome the limitations of event selectivity in the electrical power system stability analysis [14]. The proposed method utilizes high-throughput simulation automation and comprehensive contingency analysis under various inertia and disturbance conditions [15, 16]. The high-throughput simulation automation is a systematic process that generates a multitude of unique scenarios. These automations enables the execution of exhaustive contingency analysis, which in turn facilitates the application of statistical transient stability analysis for the characterization of vulnerability patterns [16]. Subsequently, the analysis reveals the existence of critical vulnerability clusters that would be impossible to identify through conventional selective approaches.

II. Methodology

A. System Model and Simulation Environment

The IEEJ EAST 10-machine system model serves as the testbed for transient stability analysis [17]. Fig. 1 illustrates the

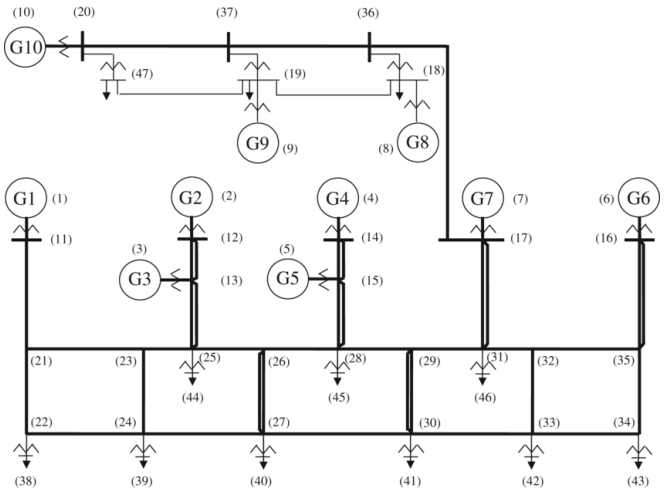

Fig. 1. IEEJ EAST 10-machine system model topology.

Table I. Generator configuration.

Number	Fuel	Capacity [MVA]	Output [MW]
G1	Thermal	8240	7000
G2		12940	11000
G3		7060	6000
G4		12940	11000
G5		7060	6000
G6		12940	11000
G7		12940	11000
G8		8240	7000
G9		8240	7000
G10		5880	5000

IEEJ EAST 10-machine system model topology. This model represents the 50 Hz eastern interconnected electrical power system in Japan, incorporating a 500 kV loop structure with underlying 275 kV networks. The system topology comprises 10 synchronous generators, 47 buses, and 61 branches with a 1000 MVA base capacity. The user can set the generator inertia constants in a random range and the contingency situations. Simulations are performed using the Central Research Institute of Electric Power Industry's (CRIEPI) Power System Analysis Tools (CPAT®).

B. *High-Throughput Simulation Framework*

The proposed workflow operates through three distinct phases, each optimized for maximum efficiency and reliability [15, 18]. The first phase involves configuring the system for different inertia levels. This process modifies generator inertia to the same value across all machines. The modified system configurations are validated to verify power flow convergence. The second phase involves defining different contingency scenarios by structuring Excel. Each excel file contains parameter definitions for disturbance type, disturbance magnitude, and fault occurrence bus. The framework features an extensible architecture for all disturbance types. The third phase implements an automated execution loop where Python systematically manages the entire simulation process [15, 19]. Each simulation case is executed in an isolated environment to

Identify applicable funding agency here. If none, delete this text box.

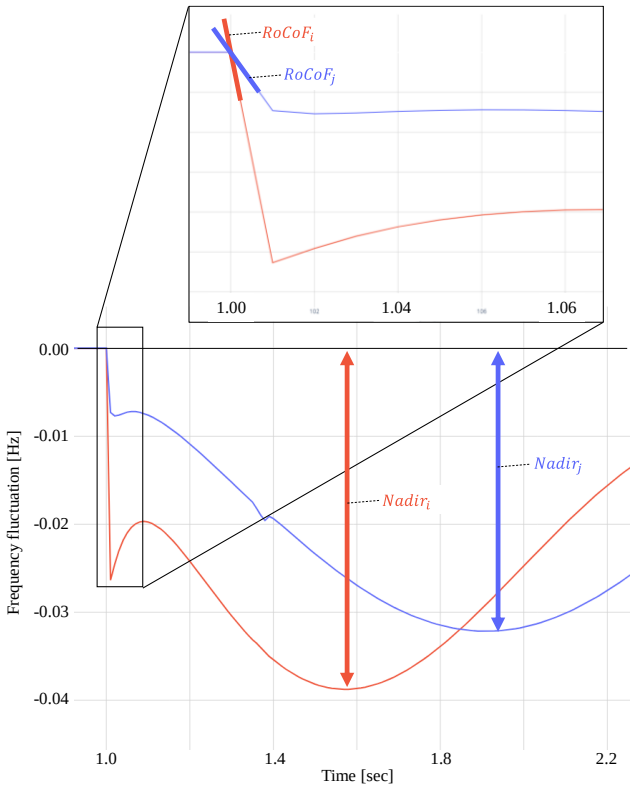

Fig. 2. An example of frequency fluctuation of the transient stability analysis.

prevent interference between scenarios. Additionally, real-time monitoring enables progress tracking, allowing for the optimization of computational resources. Finally, this framework incorporates advanced data management capabilities with automated result extraction and standardized formatting.

Manual execution of a single transient stability case in CPAT® requires approximately 90 seconds, including model loading, simulation execution, and result extraction. In contrast, the automated proposal framework reduces this time to 17 seconds per case, representing an 85% improvement [10]. Furthermore, computational efficiency is achieved through the elimination of human intervention and optimization of file I/O operations.

III. Simulation Conditions

A. *Parameter*

The generator inertia constant is set to three levels (2s, 8s, and 16s). Furthermore, the disturbance magnitude is set to 250, 500, 750, and 1000 MW, applied at 1.0s [20, 21]. The configuration of the generator is illustrated in Table 1. In this paper, the disturbance is defined as the load increase. Each bus is assigned a demand of 1890 MW.

B. *Performance Metrics*

Nadir is defined as the maximum absolute frequency deviation from 50 Hz by (1). The rate of Change of Frequency (RoCoF) is defined as the maximum magnitude of the frequency time derivative by (2). A critical measurement given

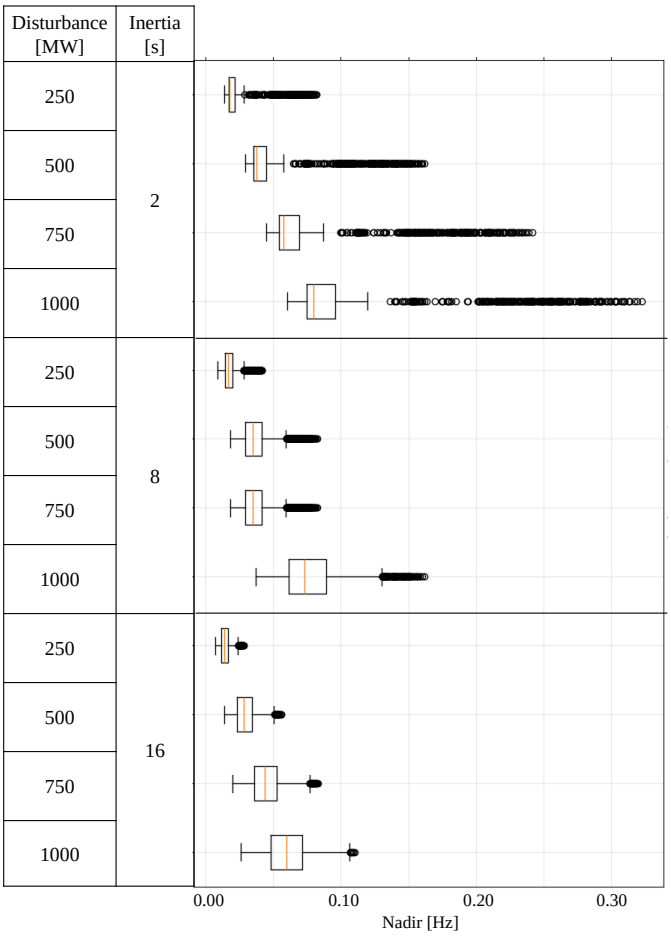

Fig. 3. Nadir for each condition.

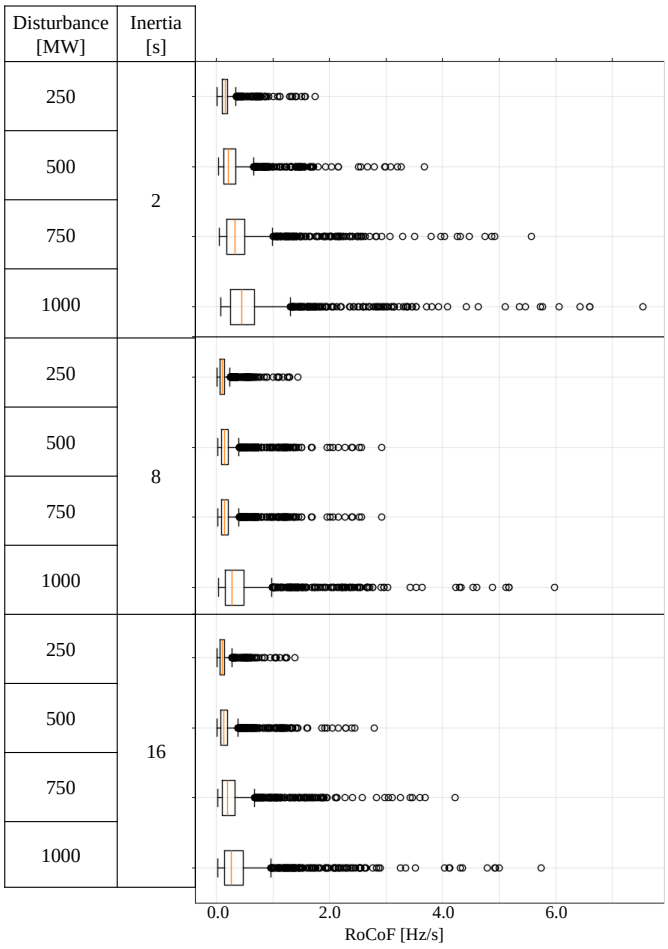

Fig. 4. RoCoF for each condition.

that high RoCoF values have been shown to trigger protective relays, leading to cascading failures [22, 23, 24].

$$nadir = \max\big(f(t)\big), \tag{1}$$

$$rocof = \max\left(\left|\frac{f(t+\Delta t) - f(t)}{\Delta t}\right|\right), \tag{2}$$

where t is time [msec] and $f(t)$ is frequency fluctuations. Δt is 10 msec.

IV. Results and Discussion

A. *Principles of Transient Stability Analysis*

Fig. 2 shows the frequency fluctuation of the transient stability analysis. The Rocof is predominantly the frequency fluctuation at the moment of the accident at 1.0s. It can be confirmed that the level of Nadir and RoCoF changes for each node, and the time period covered also changes.

B. *System Wide Performance Assessment*

Fig. 3 and Fig. 4 illustrate the box plots of Nadir and RoCoF for each scenario. Firstly, in the case of the same inertia and a different disturbance magnitude, as illustrated in Fig. 3, the range of nadir increased proportionally with the disturbance magnitude. Under low-inertia conditions (M=2.0s), the median nadir increases from 0.018 Hz (ΔP=250MW) to 0.080 Hz (ΔP=1000MW). For high-inertia systems (M=16s), the corresponding increase is from 0.014 Hz to 0.060 Hz. Next, in the case of the difference in inertia and same disturbance magnitude, under small disturbance conditions (ΔP=250MW), the median values show minimal differences across inertia levels: 0.018 Hz (M=2s), 0.017 Hz (M=8s), and 0.014 Hz (M=16s). However, the outlier characteristics differ dramatically. The low-inertia system demonstrates outliers reaching 0.082 Hz. On the other hand, under the high inertia system, the maximum outlier is limited to 0.028 Hz, representing a 2.9-fold reduction in extreme vulnerability cases. For larger disturbance magnitude (ΔP=1000MW), both median and outlier show systematic improvement with inertia enhancement. The median nadir decreases from 0.080 Hz (M=2s) to 0.060 Hz (M=16s). In comparison, the maximum outliers reduce from 0.323 Hz to 0.110 Hz. This ensures comprehensive protection across all vulnerability levels. Finally from Fig. 3, RoCoF analysis corroborates this trend with even more pronounced differences. In normal conditions (M=8s, ΔP=500MW), the median RoCoF is 0.15 Hz/s, with outliers reaching 2.92 Hz/s. In contrast, the low inertia condition (M=2s, ΔP=500MW) shows a median of 0.21 Hz/s with extreme outliers of 3.67 Hz/s, representing a 1.4-fold increase in median response and 1.3-fold increase in extreme vulnerability.

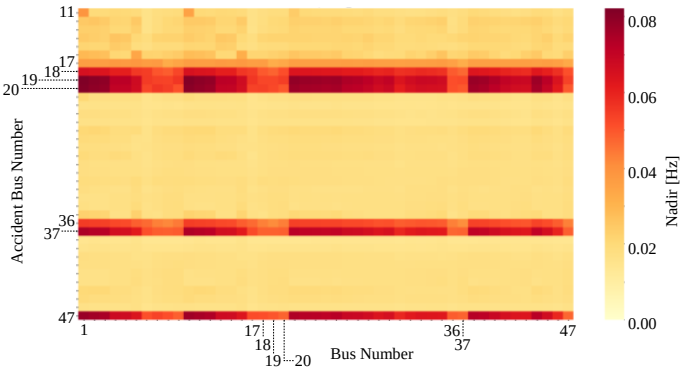

(a) M=2.0s, ΔP=250MW.

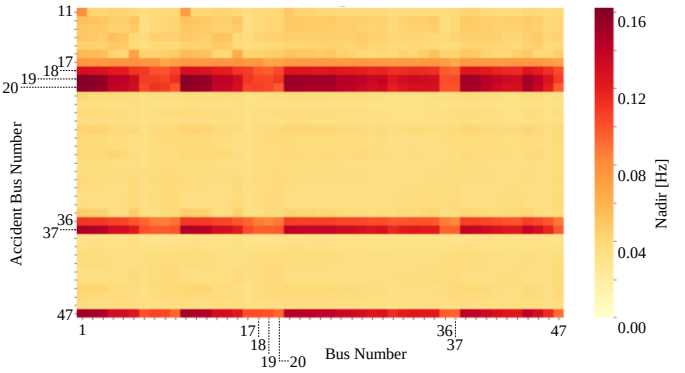

(b) M=2.0s, ΔP=500MW.

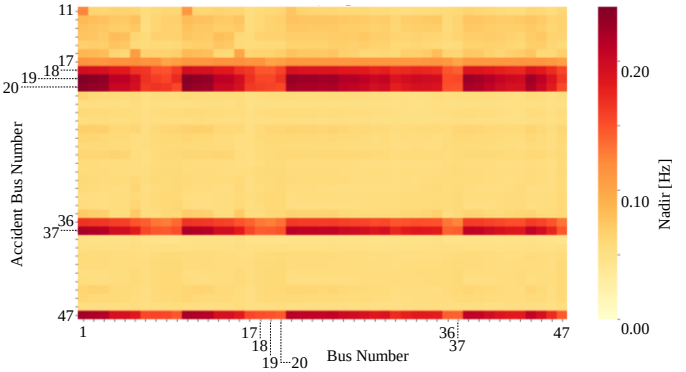

(c) M=2.0s, ΔP=750MW.

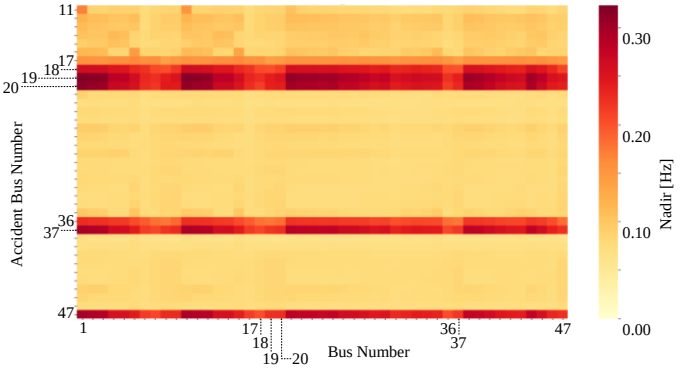

(d) M=2.0s, ΔP=1000MW.

Fig. 5. Nadir for each contingency event and each system.

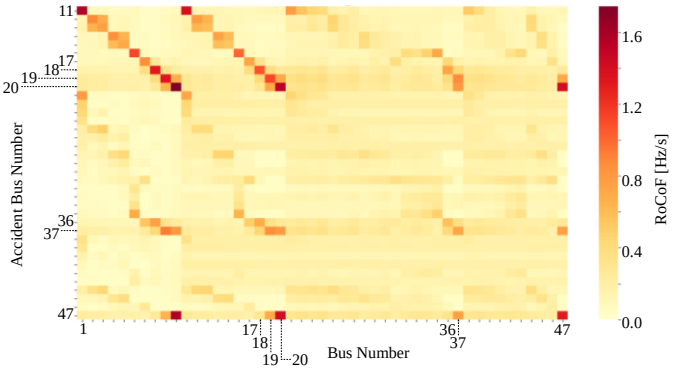

(a) M=2.0s, ΔP=250MW.

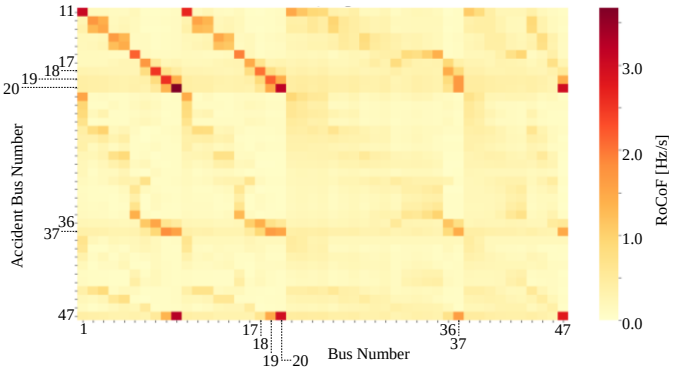

(b) M=2.0s, ΔP=500MW.

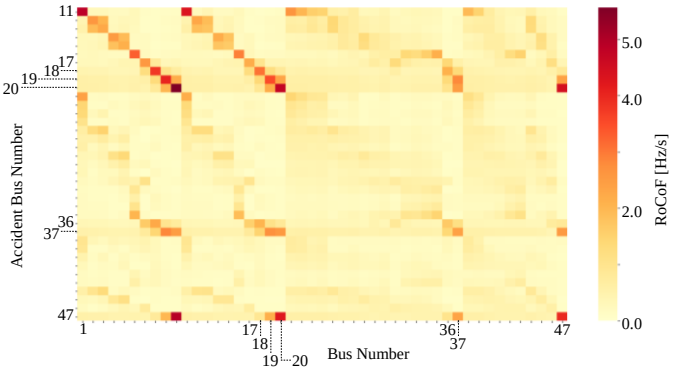

(c) M=2.0s, ΔP=750MW.

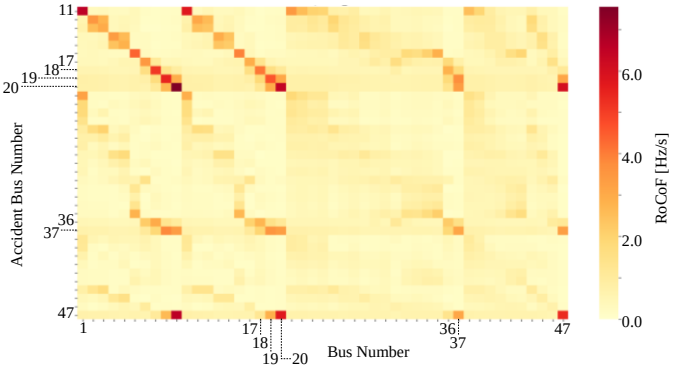

(d) M=2.0s, ΔP=1000MW.

Fig. 6. RoCoF for each contingency event and each system.

C. Spatial Vulnerability Analysis

Fig. 5 and Fig. 6 present the Nadir and RoCoF that were calculated with each distribution for inertia 2.0s. This analysis reveals distinct clustering patterns that persist across different operating conditions. According to Fig. 5, the events at buses 18, 19, 20, 36, 37, and 47 also exhibit high vulnerability levels. These six buses account for the most severe whole-system impacts, regardless of the specific disturbance magnitude or inertia level. This knowledge represents a critical vulnerability cluster that would be impossible to identify through conventional selective analysis. In addition, the distribution patterns of system impacts remain relatively unchanged. From Fig. 6, RoCoF results clarified even more pronounced spatial heterogeneity with fundamentally different characteristics compared to nadir measurements. A comparison of Fig. 5(a) and Fig. 6(a) reveals that the identical system (M=2s, ΔP=250MW) demonstrates highly localized impacts. This knowledge is clarified by analyzing the IEEJ EAST 10 machine model topology. The most vulnerable buses (buses 18, 19, 20, 36, 37, 47) are characterized by their significant electrical proximity to the generation (buses 1-10). Furthermore, these buses are localized to the fault occurrence bus and its immediate vicinity. Hence, these buses exhibit a considerable deviation and a rapid fluctuation in response to load disturbances. This finding is a quantitative assessment of an essential aspect of the electrical power system vulnerability, a fanciful view that has been said without conventional analysis.

Finally, the nadir assessment suggests that these buses should primarily prevent a contingency. At the same time, the extreme locality of the RoCoF indicates the buses that should be prioritised for countermeasures when the assumed accident occurs. These results underscore the importance of analysing both indicators to develop effective strategies for strengthening the electrical power system [26]. The identification of these topology-dependent vulnerability patterns means that a comprehensive analysis is needed, not just a simulation defined as a worst-case scenario.

V. Conclusion

The energy transition is fundamentally altering power system characteristics, reducing system inertia and increasing vulnerability. Traditional transient analysis faces significant limitations that are scenario-selective. Therefore, this paper presented a comprehensive data-driven method that addresses event selectivity limitations in the electrical power system stability analysis through high-throughput simulation automation. The automated framework achieved an 85% improvement in computational efficiency while enabling the systematic exploration of the entire contingency scenario. As a result, key findings included the identification of critical vulnerability clusters at specific buses (18, 19, 20, 36, 37, 47). Additionally, the consistent clustering of vulnerabilities across operating conditions suggested that electrical proximity to the generator has a significant influence on system response characteristics. In the future, this high-throughput simulation framework will be utilized to generate extensive big databases for machine learning [25]. Then, a method is developed to optimize inertia resource placement and capacity allocation using a database [26].

References

[1] C. He et al., "Analysis and control of frequency stability in low-inertia power systems: A review," IEEE/CAA J. Autom. Sinica, vol. 11, no. 12, pp. 2363–2383, Dec. 2024.

[2] Y. Li et al., "Artificial intelligence-based methods for renewable power system operation," Nature Rev. Elect. Eng., vol. 1, no. 1, pp. 163–179, Mar. 2024.

[3] M. O. Qays et al., "System strength shortfall challenges for renewable energy-based power systems: A review," Renew. Sustain. Energy Rev., vol. 183, p. 113447, Aug. 2023.

[4] C. He, X. He, H. Geng, et al., "Transient stability of low-inertia power systems with inverter-based generation," IEEE Trans. Energy Convers., vol. 37, no. 4, pp. 2903–2913, Dec. 2022.

[5] T. Ackermann et al., "Dynamic characteristics of low-inertia power systems: A comprehensive review," Renew. Sustain. Energy Rev., vol. 156, p. 111964, Mar. 2022.

[6] H. T. Nguyen, G. Yang, A. H. Nielsen, and P. H. Jensen, "Combination of synchronous condenser and synthetic inertia for frequency stability enhancement in low-inertia systems," IEEE Trans. Sustain. Energy, vol. 10, no. 3, pp. 997–1005, Jul. 2019.

[7] AEMO, "Black system South Australia 28 September 2016," Final Report, Mar. 2017.

[8] K. Moustakas et al., "A review of recent developments in renewable and sustainable energy systems," Renew. Sustain. Energy Rev., vol. 119, p. 109418, Mar. 2020.

[9] M. I. Saleem, S. Saha, T. K. Roy, et al., "Assessment and management of frequency stability in low inertia renewable energy rich power grids," IET Gener. Transm. Distrib., vol. 18, no. 3, pp. 456–469, Feb. 2024.

[10] M. Massaoudi, T. Zamzam, M. E. Eddin, et al., "Fast transient stability assessment of power systems using optimized temporal convolutional networks," IEEE Open J. Power Electron., vol. 5, pp. 825–838, 2024.

[11] L. Zhu, D. J. Hill, and C. Lu, "Hierarchical deep learning machine for power system online transient stability prediction," IEEE Trans. Power Syst., vol. 35, no. 3, pp. 2399–2411, May 2020.

[12] M. Senyuk et al., "Power system transient stability assessment based on machine learning algorithms and grid topology," Mathematics, vol. 11, no. 3, p. 525, Feb. 2023.

[13] IEEE/CIGRE Joint Task Force, "Definition and classification of power system stability," IEEE Trans. Power Syst., vol. 19, no. 3, pp. 1387–1401, Aug. 2004.

[14] Q. Wang, F. Li, Y. Tang, and Y. Xu, "Integrating model-driven and data-driven methods for power system frequency stability assessment and control," IEEE Trans. Power Syst., vol. 34, no. 6, pp. 4647–4658, Nov. 2019.

[15] J. Zhang et al., "High-throughput simulation framework for large-scale power system analysis," IEEE Trans. Power Syst., vol. 38, no. 2, pp. 1234–1245, Mar. 2023.

[16] R. Chen et al., "Statistical methods for power system stability assessment under uncertainty," IEEE Trans. Power Syst., vol. 37, no. 4, pp. 2890–2901, Jul. 2022.

[17] IEEJ Technical Committee, "Standard models for power system studies," IEEJ Trans. Power Energy, vol. 123, no. 4, pp. 456–467, Apr. 2003.

[18] F. De Caro, A. J. Collin, G. M. Giannuzzi, et al., "Review of data-driven techniques for on-line static and dynamic security assessment of modern power systems," IEEE Access, vol. 11, pp. 131528–131545, Nov. 2023.

[19] W. Ahmed et al., "Machine learning based energy management model for smart grid and renewable energy districts," IEEE Access, vol. 8, pp. 185059–185078, Oct. 2020.

[20] P. Zhou et al., "Reliability and economic evaluation of power system with renewables: A review," Renew. Sustain. Energy Rev., vol. 58, pp. 537–547, May 2016.

[21] A. A. Bazmi and G. Zahedi, "Sustainable energy systems: Role of optimization modeling techniques in power generation and supply," Renew. Sustain. Energy Rev., vol. 15, no. 8, pp. 3480–3500, Oct. 2011.

[22] A. Fernandez et al., "Rate of change of frequency measurement and analysis in modern power systems," IEEE Trans. Smart Grid, vol. 13, no. 3, pp. 2156–2167, May 2022.

[23] H. Yin, W. Qiu, Y. Wu, et al., "Field measurement and analysis of frequency and RoCoF for low-inertia power systems," IEEE Trans. Instrum. Meas., vol. 72, pp. 1–12, 2023.

[24] G. Rietveld, P. S. Wright, and A. J. Roscoe, "Reliable rate-of-change-of-frequency measurements: Use cases and test conditions," IEEE Trans. Instrum. Meas., vol. 69, no. 7, pp. 4525–4533, Jul. 2020.

[25] T. Meridji et al., "A power system stability assessment framework using machine-learning," Elect. Power Syst. Res., vol. 214, p. 108849, Jan. 2023.

[26] Q. Wang et al., "Integrating model-driven and data-driven methods for power system frequency stability assessment and control," IEEE Trans. Power Syst., vol. 34, no. 6, pp. 4647–4658, Nov. 2019.

Authors' background

Your Name	Title*	Research Field	Personal website
Keito Nishida	Phd candidate		
Ryuto Shigenobu	assistant professor		
Akiko Takahashi	associate professor		
Masakazu Ito	full professor		

*This form helps us to understand your paper better, the form itself will not be published.

*Title can be chosen from: master student, Phd candidate, assistant professor, lecture, senior lecture, associate professor, full professor